Journal of Harbin Engineering University
ISSN: 1006-7043

Vol 46 No. 3
March 2025

Optimization of Independent Factors Influencing the Combustion Characteristics of Carbonized Rice Husk briquettes in a Fixed-Bed Reactor Under Oxy-Fuel Conditions

John Akema, Robert Kiplimo, Peter Obara Oketch, Josephat Kipyegon Tanui

Department of Mechanical and Mechatronic Engineering, Pan-African University, Institute for Basic Sciences, Technology and Innovation, Nairobi, 6200-00200.
Department of Marine Engineering and Maritime Operation, Jomo Kenyatta University of Agriculture and Technology, P.O. Box 62000 – 00200, Nairobi, Kenya.
Department of Mechanical Engineering, Jomo Kenyatta University of Agriculture and Technology, P.O. Box 62000 – 00200, Nairobi, Kenya.

Department of Mechanical Engineering, Dedan Kimathi University of Technology, Private Bag 10143, Nyeri, Kenya.

Abstract

This research aimed to optimize the independent variables affecting the combustion characteristics of carbonized rice husk briquettes during fixed bed combustion in an oxy-fuel condition. The optimization of oxy-fuel mass flux, binder ratio, and oxy-fuel ratio (O_2/CO_2) was conducted in relation to average flame propagation speed, average burning rates, average thickness of the reaction zone, peak flame temperature, and ignition time through the use of response surface methodology (RSM). A total of seventeen distinct experiments were carried out utilizing combinations of oxy-fuel mass flow rates and ratios of binder and oxy fuel (oxygen to carbon dioxide) at three levels established by the Box Behnken Design method, a technique employed in response surface methodology (RSM). The ratio of oxy-fuel and the mass flow rate had the greatest effect on the combustion characteristics for all fuel samples. The optimal values for oxy-fuel mass flux, binder ratio, and oxy-fuel ratio were found to be 0.108 $kg/m^2\,.\,s$,4.8 wt%, and 29.4% $O_2/\ 70.6\ \%\ CO_2$, respectively. The ignition time was measured at 243 seconds, with the reaction zone thickness averaging 254 mm and a peak optimal flame temperature of 1246°C. The maximum flame propagation speed and burning rate were determined to be 0.3169 mm/s and 0.046 $kg/m^2\,.\,s$ respectively.

Keywords: Oxy-fuel ratio;O_2/CO_2;combustion; RSM, BBD; Fixed bed reactor; carbonization; Briquettes; Rice husks, optimization.

1. Introduction

As the globe confronts energy deficits and ecological h arm, scientists are swiftly investigating alternative sust ainable energy options. For instance, Africa's energy u sage is rising at twice the rate of many other regions gl obally. The 2022 report on Africa's energy prospects e mphasizes that Africa accounts for under 6% of global energy use and only 2% of total global emissions [1].

To meet this growing demand responsibly, the advanc ement of unconventional energy technologies has em erged as a significant area of international research. A notable technology with potential is oxyfuel combusti on, which consists of burning fuel using a blend of pur e oxygen and recycled flue gases rather than using am bient air. This method improves combustion efficiency while also aiding in the capture of carbon dioxide CO_2 leading to decreased greenhouse gas emissions.

The application of oxyfuel technology in biomass ener gy systems, like the burning of carbonized rice husk bri quettes, could improve the environmental advantages of biomass utilization. Biomass, currently providing mo re than 14% of global energy [1],can be made even more sustainable through the application of oxy-fuel combustion, reducing harmful emissions such as nitrogen oxides (NO_x) and particulates, while also enabling easier carbon capture.

Oxy-fuel combustion offers a pathway to carbon-neutral energy production by combining the advantages of biomass renewability, affordability, and carbon neutrality with advanced combustion technologies that minimize emissions and improve energy efficiency [2]. As Africa seeks to balance its growing energy needs with environmental stewardship, the adoption of innovative technologies like oxy-fuel combustion could play a pivotal role in achieving sustainable energy goals.

Charcoal production in sub-Saharan Africa contributes approximately 65% of global output, with 40% exported to Europe, largely for barbecues [3], [4]. Consequently, the need to research alternate sources of biomass,

including farming waste, urban solid waste, and crops energy to decrease forests destruction while enhancing conservation of environment is increasing. The expected population rise in Africa may further intensify demand on wood biomass due to anthropogenic activities. In Kenya, rural areas presently consume above 90% of nation's energy, mostly supplied from firewood and charcoal, adding to roughly 4.5 million tons every year [5]. This excessive reliance on forest biomass has led to considerable environmental challenges, including the deterioration of regions to catch water and decreasing volumes of water in water bodies, both of which are vital for electricity generation. Agriculture, an important sector in Kenya's economy, contributes for 35% of the country's Gross Domestic Product (GDP) [6]. As reported by Kimutai et al. [6], Kenya has the capacity to produce roughly 187,000 TJ of energy yearly from an estimated 13,913,223 tons of agricultural leftovers. On a global scale, Ajimotokan et al. [2] expect that agricultural residue output might reach 2×10^{12} tons annually. Waste from agriculture, being abundant, accessible, and sustainable, can be turned into pelletized fuels to compensate the dwindling supply of forest biomass.

The making of pellet fuels from agricultural waste often requires a binder to improve compactness. Research has considered utilizing cassava starch and clay [7], molasses [5], carboxymethyl cellulose, and calcium lignosulfonate [8] as binders to enhance the physical and chemical properties of these fuels. These contribute to durability and hold particles together through making stable, non-evaporative components. However, some binders, like kaolin, reduce the calorific value due to their non-combustible properties [1]. The binder amount influences fuel density, impacting biofuel performance overall. Flame front velocity and specific fuel consumption are influenced by the binder-to-fuel ratio; low-density biomass fuels usually have a faster flame front velocity compared to denser fuels due to their lower packing allowing for improved reactivity and radiative heat penetration [9].

The making of pellet fuels from agricultural waste often requires a binder to improve compactness. Research has considered utilizing cassava starch and clay [7], molasses [5], carboxymethyl cellulose, and calcium lignosulfonate [8] as binders to enhance the physical and chemical properties of these fuels. These contribute to durability and hold particles together through making stable, non-evaporative components. However, some binders, like kaolin, reduce the calorific value due to their non-combustible properties [1]. The binder amount influences fuel density, impacting biofuel performance overall. Flame front velocity and specific fuel consumption are influenced by the binder-to-fuel ratio; low-density biomass fuels usually have a faster flame front velocity compared to denser fuels due to their lower packing allowing for improved reactivity and radiative heat penetration [9].

Briquettes are commonly made using either low- or high-pressure processes for compaction, with the latter being more costly. In high-compaction procedures, production entails adding water before pressing biomass at enough pressure and temperature using reciprocating piston within a mold. Holubcik et al. [10] Characterize the compaction process as including dividing, smashing, dehydrating, forming into pellets, cooling, storing and conveying. In Africa, a widely utilized method for densifying agricultural leftovers is low-pressure briquetting and pelleting (<7 MPa). This method typically involves carbonizing agricultural waste, adding a binder, and then compacting it for cohesion [11]. Using a screw extruder minimizes energy contributions from electricity, thermal, and chemical sources. During carbonization, biomass undergoes pyrolysis at temperatures between 400℃ to 500℃ with limited oxygen, transforming into carbon. This enrichment increases higher heating value (HHV) with rising temperatures, sometimes approaching that of coal. Low-pressure methods are often used in Africa due to their reduced cost and accessibility, making them Ideal for farmers, young people, and women's organizations.

Combustion in stationary biomass systems is influenced by different factors, categorically classified into fuel morphology, composition, and operational conditions [12]. Researchers have studied each factor independently to understand its role in fixed-bed combustion processes. Mahapatra [13] highlighted that these components are interrelated, misleading findings based on single aspects. For instance, flame propagation is regulated by airflow, combustion and heat transfer, which depend on the porosity, fuel density, particle size, thermal conductivity, calorific value, moisture and ash content [13].

The processing of pelletized fuels often involves incorporating non-combustible binders, which may exacerbate issues in biomass combustion furnaces and boilers, including corrosion, agglomeration, and fouling. These challenges can result in inadequate mixing of oxy-fuel, low thermal efficiency, and uncompleted combustion since the ignition temperature might not be reached. In these cases, carbon and hydrogen may not completely oxidize to carbon dioxide and water, resulting in the release of toxic carbon monoxide. These issues have emphasized the need for increased expenses in the cleaning and

upkeep of combustion chambers. The burning characteristics of pelletized rice husk farm waste fuels have not been thoroughly studied in reactor setups to comprehend the effects of different binders on particular biofuel attributes like combustion rate, oxygen proportion, temperature trends, emissions, and flame speed at different oxygen concentrations. The traits described can help identify biomass fuels that have high ignitability, low ash levels, greater energy density, and additional beneficial fuel properties. Furthermore, it is crucial to evaluate the impact of oxy-fuel on briquette combustion by analyzing changes in binder concentrations and combustion conditions.

This study examines the impact of oxy-fuel on flame propagation speeds, reaction zone thickness, ignition time, peak flame temperature, and burning rates by evaluating oxy-fuel mass flow, molasses binder ratio, and oxy-fuel ratio. These combustion characteristics enable the assessment of fuel combustion efficiency, calorific values, energy density, ignitability, and ash reduction. This study employs the Box-Behnken Design (BBD), a method from response surface methodology (RSM), to develop optimized combustion parameters and fuel properties for enhanced efficiency and improved energy density. Through analysis of variance (ANOVA) and regression analysis (RA), major independent factors contributing to enhanced combustion properties were identified, resulting in improved combustion characteristics like average flame propagation speed, average burning rate, reaction zone thickness, maximum flame temperature, and ignition time. Subsequently, a mathematical model was created to predict these combustion characteristics utilizing the provided data.

Thika Town, Kiambu County, Kenya, were used to improve the strength of the briquettes.

The dried rice husks were carbonized in a steel drum with a height-to-diameter ratio of 2:1, featuring air control holes to regulate the pyrolysis process. This setup extended the residence time, enabling effective conversion of biomass into biochar. To maintain carbonization for four hours, the air holes were sealed with mud to limit oxygen flow, and the temperature was controlled between 400°C and 500°C to optimize the balance between biochar yield and quality [14]. Prior to carbonization, the biomass was threshed and sieved, selecting particles smaller than 0.3 mm for uniformity and easier handling. For optimal biochar synthesis, the holding period was increased to four hours to guarantee complete carbonization [15].

Spherical pellets measuring 35 mm in diameter were created using a screw extrusion machine from the machinery department of JKUAT, as shown in Fig. 1(b). Thereafter, all pellet samples were segmented into portions of 30 mm in length, as shown in Fig. 1(c). Unadulterated carbonized rice husks were examined, and the proportion of molasses binder was adjusted to 3.5%, 6.6%, and 9.7% by weight to improve combustion, lessen unpleasant odors while burning, and decrease environmental pollution. To guarantee the uniformity and consistency of the rice husk/molasses blend, a dilution technique with water comprising 10% of the total mixture was utilized

2. Methods

2.1 Pellets Production Process

This research obtained rice husks from farmers in Mwea, Kirinyaga, central Kenya, showcasing the viability of carbonized rice husk briquettes as an eco-friendly biomass fuel. Sugarcane molasses bought in

2.2 Fuel sample properties

This research investigated the composition and energy potential of carbonized rice husk pellets via proximate and ultimate analyses. The proximate analysis assessed

moisture content, volatile matter, fixed carbon, and ash content, providing data on the biomass's lower heating value (LHV). The research employed an oven to examine these factors, adhering to standards such as ISO 18134-2:2017-03E for moisture content, ISO 18122:2015 for ash, ISO 18123:2016-01 for volatile substances, and ASTM D-3172-73 for fixed carbon. The final assessment examined the amounts of carbon, hydrogen, nitrogen, sulfur, and oxygen utilizing a Flash Smart™ Elemental Analyzer (EA), model CHNS-O, offering a precision of 0.3 mg. The ISO 16994:2016 standard was employed to evaluate the carbon, hydrogen, nitrogen, sulfur, and oxygen content, which was determined by difference. Proximate analysis took place in the JKUAT lab, whereas the ultimate analysis was performed at the East African Laboratory in Upper Hill, Kenya. The gross calorific value of the pellets was measured with an accuracy of 0.2% using a bomb calorimeter, specifically an oxygen bomb calorimeter of the C200 type. The examination took place in the JKUAT lab in accordance with ISO 17225-6 standards to determine gross calorific value.

2.3 Experimental configuration

The experimental configuration included a stationary combustion chamber, an oxygen fuel delivery system, and devices to track combustion and emissions attributes, as illustrated in Fig.2.

(a)

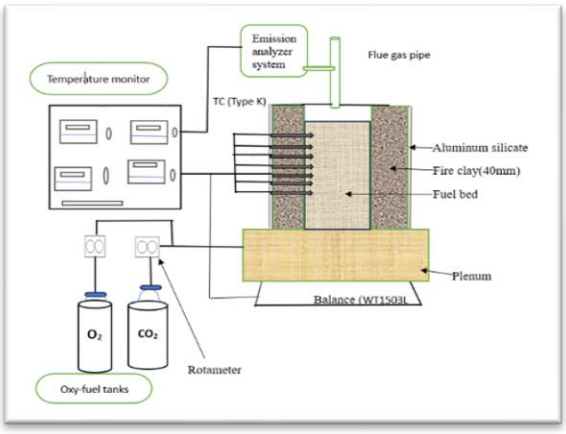

Figure 2: (a) Experimental set-up and (b) Schematic diagram.

The combustion chamber was engineered to accommodate different operating conditions, employing a fixed-bed test setup made up of five essential components: the fixed-bed gasifier, a temperature data recorder, an exhaust gas analysis system, a mass scale for carbonized rice husk pellets, and a gas flow monitoring apparatus.

A plenum chamber made of heat-resistant refractory bricks and clay was incorporated to guarantee regulated distribution of the oxy-fuel throughout the system. This plenum enabled steady oxy-fuel flow patterns, aiding in even distribution throughout the combustion chamber.

The vertical cylindrical chamber, measuring 0.540 m in height and 0.160 m in internal diameter, was constructed with four layers: an inner combustion wall, a 40 mm thickness layer of refractory cement with a heating conductivity of 0.86 W/m·K [16], a 2 mm thick mild steel plate and 18 mm thick aluminum silicate cotton fiber thermal insulation layer. The aluminum silicate cotton fiber with a thermal conductivity of 0.055 W/m·K at lower temperatures up to 400 K provided adequate thermal protection [17]. An outer radius of 276 mm was applied to the reactor, ensuring insulation in line with critical thickness requirements [18].

For the oxygen combustion system, mixture was introduced through a 1Cr18Ni9Ti stainless steel perforated plate, capable of withstanding temperatures reaching to 1400°C [18], with 66 mesh holes, each 10 millimeters in diameter. This configuration minimized air leakage and reduced turbulence within the chamber. The coefficient of convective heat transfer for forced convection.

Table 1 : Placements of thermocouples

Number of thermocouples	1	2	3	4	5	6	7
Distance measured from the base (in millimeters)	50	100	150	200	250	300	350

To monitor the fuel mass loss in the combustion chamber, an electronic scale (WT1503L) was deployed, delivering weight data to an Excel database via RS232 cable. Flexible pipe connections were built to minimize interference with the scale's measurements. Type-K thermocouples were positioned at 50 mm intervals in the cylindrical combustion chamber to oversee temperature and identify the rates at which important reaction fronts, such as drying, devolatilization, and char oxidation, progress, as described in **Table1**. The decision to use Type-K thermocouples was supported by two main factors: they can withstand temperatures up to 1360°C, which aligns with fixed-bed combustion temperatures reaching around 1300°C[19], [20], [21], and their suitability for high-temperature environments.

Each thermocouple was equipped with a 200 mm stem to extend deep into the central axis of the fixed-bed chamber, minimizing fringe effects. Measurement uncertainties for the temperature monitoring system ranged between ±2.2°C and ±6.6°C, based on the combustion temperature of the fixed bed. A data logger (BTM-4208SD model) with 0.4°C of accuracy and a resolution of 0.1°C recorded temperature readings every 1minute across seven channels. Flow rates for oxygen and carbon dioxide were monitored using LZB-10 and LZB-25 rotameters, with ranges from 1 to 10 and 2.5 to 25 m^3/h and accuracy of 0.15 m^3/h respectively.

2.4 Determination of the characteristics of combustion

2.4.1 Average flame propagation speed ($\mathbf{U_{fps}}$)

This speed, $\mathrm{U_{fps}}$,was obtained by using the distance between neighboring thermocouples and time interval between when the neighboring thermocouples reach their peak temperatures, as indicated by **Eq. (1)**

$$\boldsymbol{U_{fps} = \frac{\Delta X}{\Delta T}} \qquad \textbf{(1)}$$

$\boldsymbol{\Delta X}$ is distance between adjacent thermocouples and $\boldsymbol{\Delta T}$ is time between the occurrence of the peak temperatures in the adjacent thermocouples.

2.4.2 Ignition Time

Ignition time refers to the time required for the reaction front to initiate at the top surface of the fuel bed. It was determined for different oxy-fuel ratios, mass flow rates and molasses binder level of 3.5%,6.6%,9.7% and constant particle size of 0.3mm. The ignition time (**tig**) is indicated by a sudden spike in temperature patterns as below in the **Fig. 3.**

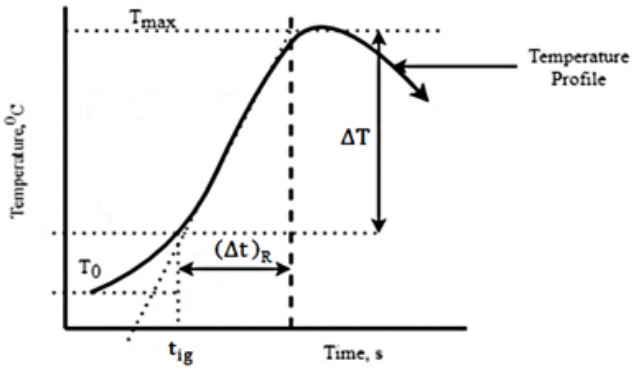

Figure 3: Diagram illustrating temperature profiles with respect to time.

In Figure 3, the flame begins to increase from the ignition temperature at time (Tig), along with a rise in flame temperature up to its maximum level. Following this peak, the flame gradually decreases as the pellets are burnt, ultimately dwindling until it extinguishes.

2.4.3 Burning rate

The fuel's burning rate denotes mass consumed by fuel over a specific time period, standardized by the cross-sectional area of the fuel bed. The combustion is considered complete when no more mass loss occurs and the temperature has greatly dropped. **Eq. (2)** illustrates a procedure that offers an aggregate value of

the process average during both the devolatilization and the char oxidation phases.

$$\dot{B_r} = \frac{\Delta m}{A * \Delta t_b} \quad (2)$$

Where $\dot{B_r}$ is burning rate, Δm is total mass of fuel consumed and Δt_b is time during devolatilization and char oxidation phases, A is the cross-section area of reactor.

2.4.4 Average reaction zone thickness

This is the distance over which the chemical reactions occur within the briquette as it undergoes combustion or other relevant processes, as expressed through **Eq. (3).**

$$X_R = U_{fps} * \Delta t_r \quad (3)$$

X_R is reaction zone thickness, U_{fps} is average flame propagation speed, Δt_r is t interval of time between the ignition time and maximum temperature for each thermocouple.

2.4.5 Peak flame temperature

This is the temperature at which the gases in the flame achieve their maximum temperature as a result of the exothermic chemical reactions that take place during combustion. Several thermocouples were placed in various locations within the flame to gather temperature profiles and assess the maximum flame temperature.

2.5 Design of experiments

In this study, a Box-Behnken design (BBD) approach was employed to find the minimal O_2/CO_2 ratio (%), mass flow rate ($kg/m^2.s$) and binder ratio (%). Both approach and a response surface methodology (RSM) assist in cost and the number of experiments reduction while determining the minimal values of combustion characteristics [18]. The number of experiments were calculated using the **Eq. (4).**

$$N = 2 * K(K-1) + CP \quad (4)$$

Where K represents the count of factors, and CP indicates the number of center points. In this research, a total of seventeen experiments were carried out, comprising twelve experiments for each factor at three levels, along with five central experiments included. Each variable was adjusted at three distinct levels with uniform intervals of (-1, 0, +1) as stipulated by BBD. Table 2 displays the independent variables: oxyfuel ratio, mass flux, and binder amount, listed from their lowest to highest range values. The classifications were designated as low, medium, and high, based on the three values for these parameters. Experimental points were generated using the BBD method with the Design-Expert 13 software.

Table 2 : Encoded independent variables [4]

Independent variables	**independent variable codes**		
	Y_1 (-1)	Y_0 (0)	Y_2 (+1)
Oxy-fuel ratio (O_2/CO_2) (%) (B)	20/80	30/70	40/60
Oxy-fuel mass flux [$Kg/(m^2.s)$] (A)	0.1	0.125	0.15
Binder ratio (%). (C)	3.5	6.6	9.7

3. Results and discussion

3.1. Experimental results

Table 3: Combustion characteristics as a function of input factors.

Run	mass flux	Oxy-fuel	Binder	Average flame propagation speed	Average Burning rate	Ignition time	Reaction zone thickness	Peak flame temperature
	$kg/m^2.s$	%	Wt%	mm/s	$kg/m^2.s$	sec	mm	℃
1	0.125	30	6.6	0.377	0.0422	240	253.995	1129.36
2	0.15	20	6.6	0.287	0.0126	240	310.149	1044.3
3	0.15	40	6.6	0.524	0.0368	120	355.422	1328.72
4	0.125	40	3.5	0.271	0.0618	240	251.031	1213.64

5	0.125	20	3.5	0.423	0.0322	300	300.954	1005.26
6	0.1	40	6.6	0.26	0.0344	175	254.208	1323.3
7	0.125	30	6.6	0.377	0.0452	240	253.995	1230.34
8	0.1	30	3.5	0.268	0.0476	235	254.796	1252.46
9	0.1	20	6.6	0.365	0.0282	240	341.512	1176.28
10	0.125	30	6.6	0.377	0.0452	240	253.995	1228.36
11	0.15	30	9.7	0.484	0.0274	180	299.644	1122.02
12	0.125	30	6.6	0.377	0.0452	240	253.995	1230.31
13	0.1	30	9.7	0.394	0.0309	240	264.891	1277.46
14	0.15	30	3.5	0.408	0.0449	235	292.591	1293.24
15	0.125	20	9.7	0.3	0.032	300	279.221	919.42
16	0.125	40	9.7	0.578	0.0338	180	286.883	1154.14
17	0.125	30	6.6	0.377	0.0432	240	253.995	1230.36

Neque laoreet suspendisse interdum consectetur libero id faucibus. Ac turpis egestas maecenas pharetra convallis. Sagittis aliquam malesuada bibendum arcu vitae elementum curabitur vitae nunc. Nulla facilisi cras fermentum odio eu feugiat

pretium nibh. Tortor at auctor urna nunc id cursus. Bibendum enim facilisis gravida neque convallis a cras semper auctor. Feugiat vivamus at augue eget arcu. Et netus et malesuada fames ac turpis egestas. Quisque id diam vel quam elementum. Amet est placerat in egestas erat. Egestas maecenas pharetra convallis posuere morbi leo. Sagittis.

The outcomes of the research indicate that the interaction between mass flux, oxy-fuel concentration, and binder percentage significantly influences the combustion characteristics of biomass briquettes, as shown in Table 3. An essential observation is the connection between mass flux and the rate of flame propagation. Experiments with higher mass flux values, like 0.125 $kg/m^2.s$ show quicker flame propagation rates. For example, run 16 reaches a maximum speed of 0.578 mm/s. This demonstrates that a higher mass flux guarantees a greater energy delivery to the combustion area, facilitating faster flame spread. Conversely, reduced mass flux values are linked to slower propagation speeds, highlighting the vital importance of mass flux in maintaining steady energy transfer throughout combustion. The combustion rate, which measures the speed of mass usage while burning, shows considerable differences across the trials. The highest burning rate of 0.06175 kg/(m²·s) (Run 4) is obtained with minimal binder content (3.5 wt%) and elevated oxy-fuel concentration (40%).

This indicates that lower binder content enhances combustion reactivity by decreasing thermal resistance, enabling more efficient oxidation of the biomass. In contrast, higher binder concentration (9.7 wt.%) appears to decrease the burning rate because its insulating properties hinder the release of volatile substances.

Ignition time, a crucial metric for evaluating the fuel's reactivity, ranges from 120 seconds (Run 3) to 300 seconds (Runs 5 and 15). The findings indicate that lower binder content significantly shortens ignition time, evident in Runs 3 and 4, where a 3.5 wt% binder leads to faster ignition. In contrast, a higher binder concentration, like 9.7 wt%, prolongs ignition times, presumably due to improved heat stability. These results highlight the necessity of modifying binder levels to achieve rapid ignition while maintaining sufficient briquette strength for handling and storage.

The thickness of the reaction zone, reflecting the geographic reach of combustion, shows moderate variation across the runs. Thicker reaction zones, like 355 mm in Run 3, are seen with high oxy-fuel concentrations (40%) and minimal binder content. This suggests enhanced oxygen accessibility and fuel reactivity, facilitating deeper engagement of combustion events. Conversely, reduced reaction zones are associated with lower oxy-fuel levels or increased binder content, suggesting constrained reaction depth.

Binder, %	Mc, %	Ac, %	Vm, %	Fc, %	Gross Cv, MJ/kg
3.5	5.40±0.22a	45.83±0.14a	18.38±0.7a	35.36±0.98a	27.12±0.21a
6.6	4.37±0.18b	47.69±0.12b	15.83±0.6b	31.97±0.84b	25.53±0.18b
9.7	3.35±0.22c	49.55±0.14c	13.28±0.69c	28.58±0.98c	23.93±0.21c
P-value	0.018	0.031	0.046	0.048	0.023

(Run 15) to 1329°C (Run 3). Peak temperatures are achieved with elevated oxy-fuel concentrations and a moderate binder content of 6.6 wt%. This emphasizes the role of oxygen enrichment in enhancing combustion intensity and thermal energy output.

The findings highlight the intricate equilibrium required to optimize combustion factors for biomass briquettes. Elevated mass flux and oxy-fuel concentration typically accelerate flame propagation speed, increase the burning rate, and raise the peak flame temperature, whereas a decrease in binder content shortens ignition time and boosts combustion efficiency. Nevertheless, trade-offs need to be managed carefully since increased binder content is crucial for maintaining structural integrity, while oxygen enrichment leads to added costs.

Table 4: Briquettes Proximate analysis (based on dry weight).

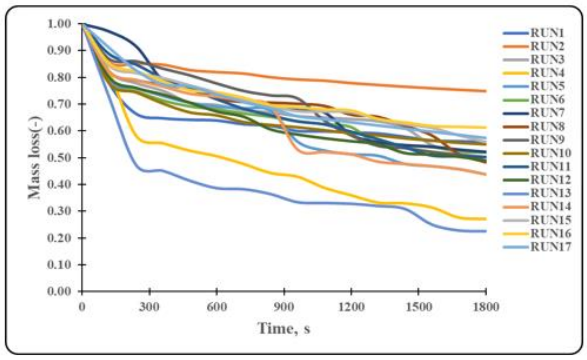

Figure 4: Fuel-bed mass loss history

The mass loss patterns of rice husk briquettes exhibit a declining trend over time, demonstrating the progress of combustion phases. The drying phase experiences a gradual rate of mass reduction, succeeded by a more significant drop during the devolatilization phase, where volatile substances are released and burned. The uniform reactions maintain the rate of mass reduction as volatiles combust in the gas phase, and a gradual decrease in mass loss takes place during the char combustion phase as the remaining carbon is oxidized.

The combustion characteristics of rice husk briquettes change significantly with alterations in oxy-fuel mass flow, binder concentration, and oxy-fuel ratio. Oxy-fuel mass flow speeds up the combustion process by supplying additional oxygen to the reaction zone, resulting in a higher burning rate and elevated peak flame temperature. An increased oxygen supply enhances the quicker and more consistent release of volatiles, while a greater binder content boosts the integrity and stability of briquettes.

The ratio of oxy-fuel significantly impacts every phase of combustion, with higher oxy-fuel levels leading to an increased oxygen concentration, which in turn raises flame temperatures and rates of reaction. This results in enhanced heat transfer throughout the drying process, promoting swift moisture evaporation. Elevated oxy-fuel ratios guarantee effective combustion of released volatiles, leading to higher flame propagation rates.

To sum up, the interplay of these factors determines the efficiency of combustion and the history of mass loss. Increased oxy-fuel mass flow and ratios lead to quicker combustion rates and elevated peak flame temperatures, whereas a greater binder content guarantees structural stability and extends the char reaction phase.

Fig.4 illustrates the mass loss trends under oxy-fuel combustion conditions. In Run13, characterized by briquette combustion at an oxy-fuel mass flow of 0.1 $\mathrm{kg/m^2.s}$, a binder ratio of 9.7 wt%, and an oxy-fuel ratio of 30%, the mass depletion curve exhibits a pronounced drop following the devolatilization phase. This differs from Run7, where combustion takes place at a higher oxy-fuel mass flux of 0.125 $\mathrm{kg/(m^2.s)}$ with

a binder ratio of 6.6% and an identical oxy-fuel ratio of 30%,

Leading to a gentler slope due to excessive flow which caused incomplete combustion, as some fuel particles did not have enough time to fully combust before being carried away by the higher oxyfuel flow [22]. The rate of combustion during devolatilization significantly shapes these curves. Lastly, the experiments showed that the burning rates initially rise quickly from mass flux of 0.125 to 0.15, before gradually declining to 0.1 $\mathrm{kg/m^2 . s}$.

3.3 Optimization of independent variables results using RSM

The emphasized forecast in **Fig. 5** illustrates the optimal values for the peak flame temperature parameter examined. This value is observed at the optimal factor levels of oxy-fuel mass flux (A) at 0.108$\mathrm{kg/m^2 . s}$, oxy-fuel ratio (B) at 29.4%, and binder ratio (C) at 4.8 wt%, reflecting near-stoichiometric conditions. This stoichiometric balance guarantees that the oxygen supplied aligns with the fuel requirements for effective combustion, reducing unburned fuel while avoiding surplus oxygen that might decrease flame temperatures or impede reactions.

The expected peak flame temperature is 1246°C, which is marginally less than the highest recorded temperature of 1351°C. This temperature is deemed optimal as it ensures a balance in combustion conditions to minimize excessive fuel usage or thermal stresses. The near-stoichiometric state guarantees adequate oxygen for full combustion, producing a high yet regulated temperature, essential for optimizing energy efficiency and preserving system stability. Conversely, in conditions of rich combustion, having too much fuel compared to oxygen might elevate the temperature further but can lead to incomplete combustion and higher emissions. In contrast, lean conditions where there is less fuel compared to oxygen would decrease the flame temperature, affecting efficiency.

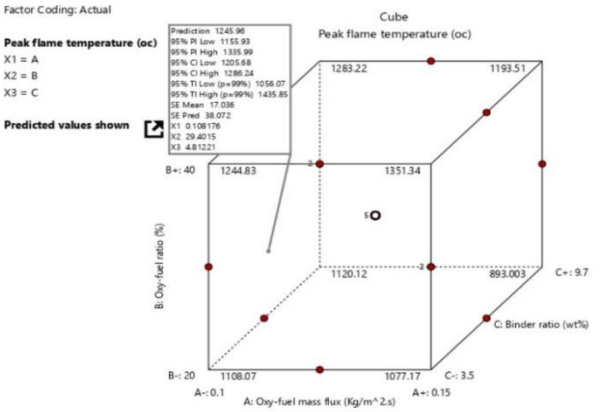

Figure 5: Optimal binder ratio, oxy-fuel ratio and oxy-fuel mass flux in relation to peak flame temperature

The emphasized forecast in **Fig. 6** illustrates the optimal values for the ignition time parameter examined. This value is observed at the optimal factor levels of oxy-fuel mass flux (A) at 0.108 $\mathrm{kg/m^2 . s}$, oxy-fuel ratio (B) at 29.4%, and binder ratio (C) at 4.8 wt%, reflecting near-stoichiometric conditions. The ignition time is 243 seconds, indicating a moderate ignition characteristic. This value guarantees that the fuel-air mixture is adequately prepared prior to the start of combustion, essential for achieving stable and efficient combustion. Under stoichiometric conditions, the ignition process is not unduly slowed down (as in lean conditions with gradual heat accumulation) nor excessively fast (as in rich conditions, where unburned fuel may create inconsistencies). The balanced levels of oxygen and binder at these settings support a dependable ignition process without undermining the thermal integrity of the system.

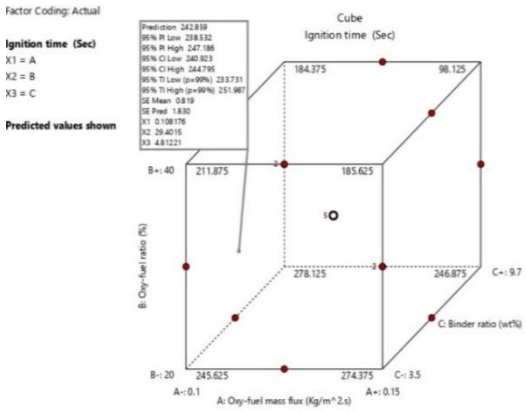

Figure 6: Optimal binder ratio, oxy-fuel ratio and oxy-fuel mass flux in relation to ignition time

The emphasized forecast in **Fig. 7** illustrates the optimal values for the average flame propagation speed parameter examined. This value is observed at the optimal factor levels of oxy-fuel mass flux (A) at 0.108 $\mathrm{kg/m^2 . s}$, oxy-fuel ratio (B) at 29.4%, and binder ratio

(C) at 4.8 wt%, reflecting near-stoichiometric conditions. The average flame propagation speed is predicted at 0.3169 mm/s, representing a steady and controlled flame front. This speed is critical in oxy-fuel combustion, as it ensures consistent heat transfer and reaction stability. In lean conditions, the propagation speed would likely decrease due to reduced fuel availability, leading to slower reaction rates. On the other hand, rich conditions might increase propagation speed but could result in flame instability or localized overheating. The near-stoichiometric factor levels ensure an optimal propagation speed, balancing reaction stability and combustion efficiency.

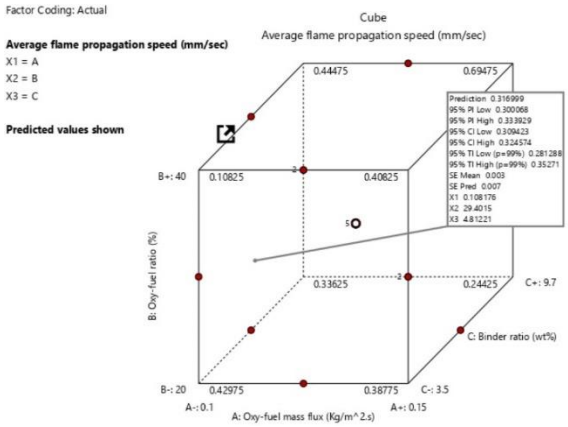

Figure 7: Optimal binder ratio, oxy-fuel ratio and oxy-fuel mass flux in relation to average flame propagation speed

Fig. 8 illustrates the anticipated thickness of the reaction zone (253.616 mm) under optimal combustion conditions. The optimal input values needed to obtain the forecasted reaction zone thickness are Oxy-fuel mass flux: 0.108 $\mathrm{kg/m^2.s}$, Oxy-fuel ratio: 29.4%, and Binder ratio: 4.8 wt%. These values suggest that the combustion process takes place with a precise balance of fuel and oxidizer, essential for the thickness of the reaction zone. The oxy-fuel ratio offers essential information about the combustion process, as it indicates if the conditions are lean, stoichiometric, or rich. At 29.4%, the oxygen level is probably refined for stoichiometric combustion, where the fuel and oxidizer are proportioned to reach full combustion. This condition reduces fuel waste and enhances energy efficiency, aiding in achieving an ideal thickness for the reaction zone.

Conversely, lean combustion, marked by a surplus of oxygen, would lead to a thinner reaction zone as a result of diminished fuel supply and slower reaction speeds. On the other hand, rich combustion, in which the fuel surpasses the available oxygen, may lead to an increase in reaction zone thickness caused by incomplete combustion and the creation of unburned intermediates. The stoichiometric condition reached here guarantees a stable and efficient combustion process, creating the expected reaction zone thickness based on the specified oxy-fuel mass flux and binder ratio.

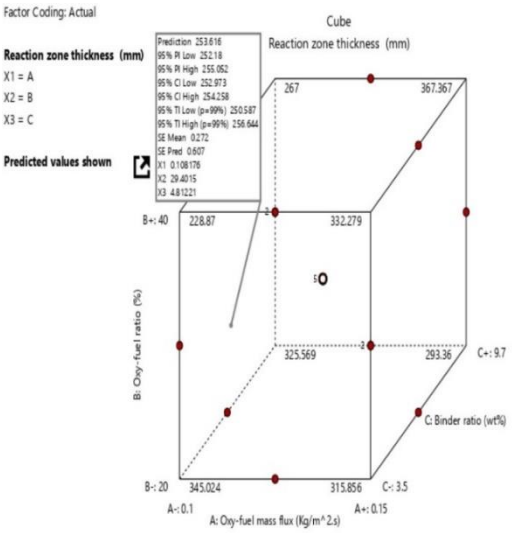

Figure 8: Optimal binder ratio, oxy-fuel ratio and oxy-fuel mass flux in relation to reaction zone thickness.

Fig.9 illustrates average burning rate of 0.046 $\mathrm{kg/m^2.s}$, realized under optimal combustion conditions characterized by an oxy-fuel mass flux of 0.108 $\mathrm{kg/m^2.s}$, an oxy-fuel ratio of 29.4%, and a binder ratio of 4.8 wt%. The oxy-fuel ratio of 29.4% indicates that the combustion process is nearly at stoichiometric conditions, meaning the fuel-to-oxygen ratio is balanced to achieve complete combustion. This equilibrium optimizes energy output, producing a high and consistent burn rate while reducing unburned fuel or surplus oxygen waste.

In contrast, with lean combustion where the oxygen availability surpasses the stoichiometric need—the combustion rate is likely to decline. This happens as the additional oxygen dilutes the reaction area, decreasing fuel concentration and slowing the reaction kinetics. Conversely, rich combustion with more fuel than the available oxygen can also slow the burning rate due to incomplete combustion, resulting in unburned fuel and lower energy efficiency. Both lean and rich conditions lead to suboptimal combustion rates and reduced thermal efficiency when compared to stoichiometric combustion. The anticipated burning rate of 0.046 $\mathrm{kg/m^2.s}$, reached under the ideal conditions, signifies a well-balanced and effective combustion process.

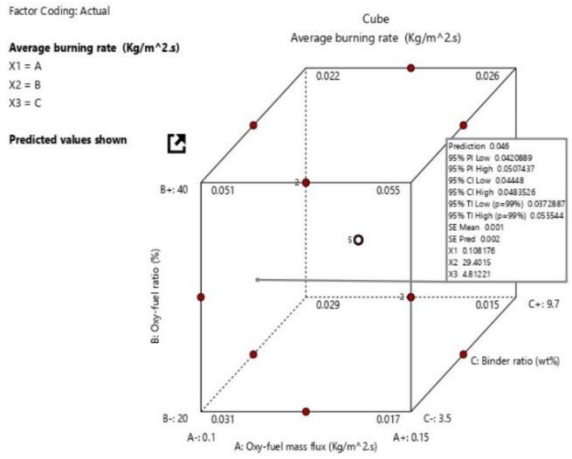

Figure 9: Optimal binder ratio, oxy-fuel ratio and oxy-fuel mass flux in relation to average burning rate

In the end, Optimization was conducted to identify a blend of three components and create fuel with enhanced combustion properties compared to combustion in air. The research improved the oxy-fuel ratio, oxy-fuel mass flux, and binder ratio as input factors to evaluate the thermal efficiency of the briquette. An optimal ignition time of 243 seconds was obtained, while the ideal average reaction zone thickness was reached at 254 mm, utilizing the optimal parameters of an oxy-fuel mass flux of 0.108 $\mathrm{kg/m^2}$.s, a binder mass of 4.8wt% molasses, and an oxy-fuel ratio of 29.4% O_2 / 70.6% CO_2 . Moreover, the maximum ideal temperature attained by the flame and the average speed of its propagation were recorded at 1246 °C and 0.3169 mm/s, respectively, with the mass flux of the oxy-fuel fixed at 0.108 $\mathrm{kg/m^2}$.s. This was achieved by utilizing an optimal binder ratio of 4.8 wt% molasses and an optimal oxy-fuel ratio of 29.4%, along with a mass flux of 0.108 $\mathrm{kg/m^2}$.s. In the end, the maximum optimal burning rate reached was 0.046 $\mathrm{kg/m^2}$.s, with an oxy-fuel ratio of 29.4%, an oxy-fuel mass flow of 0.108 $\mathrm{kg/m^2}$.s, and a binder proportion of 4.8 wt%.

4. Conclusion

This research examined the impact of oxy-fuel mass flow, binder ratio, and oxy-fuel proportion on the combustion characteristics of carbonized rice husk briquettes. The findings demonstrated that both the mass flow rate of oxy-fuel and the oxy-fuel ratio greatly influence combustion properties, determining if the reaction is limited by oxygen availability or fuel richness depending on the oxygen level in the combustion chamber. Moreover, the research assessed the influence of the binder ratio on combustion characteristics in oxy-fuel environments. Raising the binder ratio resulted in a better average flame propagation speed, with a maximum at an ideal binder content of 9.7 wt%. Nonetheless, the average burning rate declined with a higher binder ratio, suggesting lower energy output and combustion effectiveness. The thickness of the reaction zone diminished with increased binder ratios, suggesting a more vigorous combustion process. The maximum flame temperature reached its peak at the ideal binder ratio, indicating enhanced thermal efficiency. On the other hand, ignition time rose with greater binder ratios, peaking at 9.7 wt%, as a result of the moisture level in the briquettes. These results emphasize the significance of adjusting the binder ratio to enhance combustion efficiency and emission management in the oxy-fuel combustion of rice husk briquettes.

The optimal values for oxy-fuel mass flux, binder ratio, and oxy-fuel ratio were found to be 0.108 $kg/m^2 . s$,4.8 wt%, and 29.4% O_2/ 70.6 % CO_2, respectively. The ignition time was measured at 256 seconds, with the reaction zone thickness averaging 254 mm and a peak optimal flame temperature of 1246°C. The maximum flame propagation speed and burning rate were determined to be 0.3169 mm/s and 0.046 $kg/m^2 . s$ respectively.

This study identified the optimal values for oxy-fuel mass flux, binder ratio, and oxy-fuel ratio to be 0.108 $kg/m^2 . s$, 4.8 wt%, and 29.4% O_2/ 70.6 % CO_2, respectively for the combustion characteristics of rice husk briquettes, achieving an ignition time of 243 seconds, an average reaction zone thickness of 254 mm, and a peak flame temperature of 1246 °C. The flame propagation speed was optimized at 0.3169 mm/s, and the average burning rate reached 0.046 $kg/m^2 . s$.

Credit Contribution Statement for Authorship

J. Akema: Conceptualization, Methodology, Research, Writing – Original draft. **R. Kiplimo**: Conceptualization, Methodology, Supervision. **P.O. Oketch**: Conceptualization, Methodology, Supervision. **J.K. Tanui**: Conceptualization, Methodology, Investigation, Supervision, Writing – Review & Editing.

Statement of Conflicting Interests

The authors state that there are no financial or personal conflicts of interest that may have affected the work outlined in this paper.

Acknowledgement

This study received financial backing from the Pan African University Institute for Basic Sciences, Technology, and Innovation.

References

[1] Y. H. Zheng *et al.*, "Biomass energy utilization in rural areas may contribute to alleviating energy crisis and global warming: A case study in a typical agro-village of Shandong, China," 2010, *Elsevier Ltd*. doi: 10.1016/j.rser.2010.07.052.

[2] E. D. Vicente *et al.*, "Emissions from residential pellet combustion of an invasive acacia species," *Renew Energy*, vol. 140, pp. 319–329, Sep. 2019, doi: 10.1016/j.renene.2019.03.057.

[3] C. Nabukalu and R. Gieré, "Charcoal as an energy resource: Global trade, production and socioeconomic practices observed in Uganda," *Resources*, vol. 8, no. 4, Dec. 2019, doi: 10.3390/RESOURCES8040183.

[4] "Detailed study of wood combustion in a fixed bed reactor under oxy-fuel condition josephat kipyegon tanui a thesis submitted in partial fulfilment of the requirements for the award of the degree of doctor of philosophy in mechanical engineering in the," 2020.

[5] J. K. Tanui, P. N. Kioni, P. N. Kariuki, and J. M. Ngugi, "Influence of processing conditions on the quality of briquettes produced by recycling charcoal dust," *International Journal of Energy and Environmental Engineering*, vol. 9, no. 3, pp. 341–350, Sep. 2018, doi: 10.1007/s40095-018-0275-7.

[6] J. Werther, M. Saenger, E.-U. Hartge, T. Ogada, and Z. Siagi, "Combustion of agricultural residues." [Online]. Available: www.elsevier.com/locate/pecs

[7] M. Lubwama, A. Birungi, A. Nuwamanya, and V. A. Yiga, "Characteristics of rice husk biochar briquettes with municipal solid waste cassava, sweet potato and matooke peelings as binders," *Mater Renew Sustain Energy*, vol. 13, no. 2, pp. 243–254, Aug. 2024, doi: 10.1007/s40243-024-00262-x.

[8] W. Yang *et al.*, "Effect of minerals and binders on particulate matter emission from biomass pellets combustion," *Appl Energy*, vol. 215, pp. 106–115, Apr. 2018, doi: 10.1016/j.apenergy.2018.01.093.

[9] W. Yang *et al.*, "Effect of minerals and binders on particulate matter emission from biomass pellets combustion," *Appl Energy*, vol. 215, pp. 106–115, Apr. 2018, doi: 10.1016/j.apenergy.2018.01.093.

[10] M. Holubcik, R. Nosek, and J. Jandacka, "Optimization of the Production Process of Wood Pellets by Adding Additives," *International Journal of Energy Optimization and Engineering*, vol. 1, no. 2, pp. 20–40, Apr. 2012, doi: 10.4018/ijeoe.2012040102.

[11] T. H. Mwampamba, M. Owen, and M. Pigaht, "Opportunities, challenges and way forward for the charcoal briquette industry in Sub-Saharan Africa," *Energy for Sustainable Development*, vol. 17, no. 2, pp. 158–170, 2013, doi: 10.1016/j.esd.2012.10.006.

[12] J. Porteiro, D. Patiño, J. Moran, and E. Granada, "Study of a fixed-bed biomass combustor: Influential parameters on ignition front propagation using parametric analysis," *Energy and Fuels*, vol. 24, no. 7, pp. 3890–3897, Jul. 2010, doi: 10.1021/ef100422y.

[13] S. Mahapatra and S. Dasappa, "Experiments and analysis of propagation front under gasification regimes in a packed bed," *Fuel Processing Technology*, vol. 121, pp. 83–90, May 2014, doi: 10.1016/j.fuproc.2014.01.011.

[14] J. A. Rodriguez, J. F. Lustosa Filho, L. C. A. Melo, I. R. de Assis, and T. S. de Oliveira, "Influence of pyrolysis temperature and feedstock on the properties of biochars produced from agricultural and industrial wastes," *J Anal Appl Pyrolysis*, vol. 149, Aug. 2020, doi: 10.1016/j.jaap.2020.104839.

[15] Z. Guo *et al.*, "Characteristics of biomass charcoal briquettes and pollutant emission reduction for sulfur and nitrogen during combustion," *Fuel*, vol. 272, Jul. 2020, doi: 10.1016/j.fuel.2020.117632.

[16] K. G. Fey, I. Riehl, R. Wulf, and U. Gross, "Experimental and numerical investigation of the first heat-up of refractory concrete," *International Journal of Thermal Sciences*, vol. 100, pp. 108–125, Feb. 2016, doi: 10.1016/j.ijthermalsci.2015.09.010.

[17] H. Yamashita, T. Ogami, and K. Kanamura, "Hydrothermal synthesis of hollow Al2O3 microfibers for thermal insulation materials," *Bull Chem Soc Jpn*, vol. 91, no. 5, pp. 741–746, 2018, doi: 10.1246/bcsj.20170398.

[18] P. Kipngetich, R. Kiplimo, J. K. Tanui, and P. C. Chisale, "Optimization of combustion parameters of carbonized rice husk briquettes in a fixed bed using RSM technique," *Renew Energy*, vol. 198, pp. 61–74, Oct. 2022, doi: 10.1016/j.renene.2022.07.130.

[19] S. Hermansson and H. Thunman, "Measures to reduce grate material wear in fixed-bed combustion," *Energy and Fuels*, vol. 25, no. 4, pp. 1387–1395, Apr. 2011, doi: 10.1021/ef101473b.

[20] D. Shin and S. Choi, "The Combustion of Simulated Waste Particles in a Fixed Bed," 2000.

[21] R. Johansson, H. Thunman, and B. Leckner, "Sensitivity analysis of a fixed bed combustion model," *Energy and Fuels*, vol. 21, no. 3, pp. 1493–1503, May 2007, doi: 10.1021/ef060500z.

[22] S. S. Hou, C. Y. Chiang, and T. H. Lin, "Oxy-fuel combustion characteristics of pulverized coal under O2/recirculated flue gas atmospheres," *Applied Sciences (Switzerland)*, vol. 10, no. 4, Feb. 2020, doi: 10.3390/app10041362.

[23] A. Rapheal, C. Moki, and A. Habeeb, "the effect of binder ratio on the physical and combustion characteristics of carbonized rice stalk briquettes," *| www.ijaar.org Journal International Journal of Advanced Academic Research*, vol. ISSN, no. 10, pp. 2488–9849, 2020, doi: 10.46654/ij.24889849.

[24] F. L. Sacomano Filho, L. E. de Albuquerque Paixão e Freire de Carvalho, J. A. van Oijen, and G. C. Krieger Filho, "Effects of reaction mechanisms and differential diffusion in oxy-fuel combustion including liquid water dilution," *Fluids*, vol. 6, no. 2, Feb. 2021, doi: 10.3390/fluids6020047.

[25] Z. Wang, Y. Xiong, X. Cheng, and M. Liu, "Experimental study on the flame propagation characteristics of heavy oil oxy-fuel combustion," *Journal of the Energy Institute*, vol. 92, no. 6, pp. 1630–1640, Dec. 2019, doi: 10.1016/j.joei.2019.01.011.

[26] B. Raho, G. Colangelo, M. Milanese, and A. de Risi, "A Critical Analysis of the Oxy-Combustion Process: From Mathematical Models to Combustion Product Analysis," Sep. 01, 2022, *MDPI*. doi: 10.3390/en15186514.

[27] M. Horttanainen, J. Saastamoinen, and P. Sarkomaa, "Operational limits of ignition front propagation against airflow in packed beds of different wood fuels," *Energy and Fuels*, vol. 16, no. 3, pp. 676–686, May 2002, doi: 10.1021/ef010209d.

[28] J. J. Saastamoinen, R. Taipale, M. Horttanainen, and P. Sarkomaa, "Propagation of the Ignition Front in Beds of Wood Particles," 2000.

[29] S. Mahapatra, S. Kumar, and S. Dasappa, "Gasification of wood particles in a co-current packed bed: Experiments and model analysis," *Fuel Processing Technology*, vol. 145, pp. 76–89, May 2016, doi: 10.1016/j.fuproc.2016.01.032.

[30] S. Talei, D. Fozer, P. S. Varbanov, A. Szanyi, and P. Mizsey, "Oxyfuel Combustion Makes Carbon Capture More Efficient," *ACS Omega*, 2023, doi: 10.1021/acsomega.3c05034.

[31] Y. B. Yang, H. Yamauchi, V. Nasserzadeh, and J. Swithenbank, "Effects of fuel devolatilisation on the combustion of wood chips and incineration of simulated municipal solid wastes in a packed bed," *Fuel*, vol. 82, no. 18, pp. 2205–2221, Dec. 2003, doi: 10.1016/S0016-2361(03)00145-5.

[32] Y. B. Yang, V. N. Sharifi, and J. Swithenbank, "Effect of air flow rate and fuel moisture on the burning behaviours of biomass and simulated municipal solid wastes in packed beds," in *Fuel*, Aug. 2004, pp. 1553–1562. doi: 10.1016/j.fuel.2004.01.016.

[33] S. A. El-Sayed, M. E. Mostafa, T. M. Khass, E. H. Noseir, and M. A. Ismail, "Combustion and mass loss behavior and characteristics of a single biomass pellet positioning at different orientations in a fixed bed reactor," *Biomass Convers Biorefin*, vol. 14, no. 14, pp. 15373–15393, Jul. 2024, doi: 10.1007/s13399-023-03767-z.